

## High-pressure phase diagrams of $\text{CeRhIn}_5$ and $\text{CeCoIn}_5$ studied by ac calorimetry

This article has been downloaded from IOPscience. Please scroll down to see the full text article.

2004 J. Phys.: Condens. Matter 16 8905

(<http://iopscience.iop.org/0953-8984/16/49/008>)

View [the table of contents for this issue](#), or go to the [journal homepage](#) for more

Download details:

IP Address: 129.252.86.83

The article was downloaded on 27/05/2010 at 19:24

Please note that [terms and conditions apply](#).

# High-pressure phase diagrams of CeRhIn<sub>5</sub> and CeCoIn<sub>5</sub> studied by ac calorimetry

G Knebel<sup>1</sup>, M-A Méasson<sup>1</sup>, B Salce<sup>1</sup>, D Aoki<sup>1</sup>, D Braithwaite<sup>1</sup>,  
J P Brison<sup>2</sup> and J Flouquet<sup>1,3</sup>

<sup>1</sup> Département de Recherche Fondamentale sur la Matière Condensée, SPSMS, CEA Grenoble, 38054 Grenoble Cedex 9, France

<sup>2</sup> Centre de Recherche sur les Très Basses Températures, CNRS, 38042 Grenoble Cedex 9, France

<sup>3</sup> Institut de Physique de la Matière Condensée de Grenoble, 38042 Grenoble Cedex 9, France

E-mail: gknebel@cea.fr

Received 2 August 2004

Published 26 November 2004

Online at [stacks.iop.org/JPhysCM/16/8905](http://stacks.iop.org/JPhysCM/16/8905)

doi:10.1088/0953-8984/16/49/008

## Abstract

The pressure–temperature phase diagrams of the heavy fermion antiferromagnet CeRhIn<sub>5</sub> and the heavy fermion superconductor CeCoIn<sub>5</sub> have been studied under hydrostatic pressure by ac calorimetry and ac susceptibility measurements using diamond anvil cells with argon as the pressure medium. In CeRhIn<sub>5</sub>, the use of a highly hydrostatic pressure transmitting medium allows for a clean simultaneous determination by a bulk probe of the antiferromagnetic and superconducting transitions. We compare our new phase diagram with the previous ones, discuss the nature (first or second order) of the various lines, and the coexistence of antiferromagnetic order and superconductivity. The link between the collapse of the superconducting heat anomaly and the broadening of the antiferromagnetic transition points to an inhomogeneous appearance of superconductivity below  $P_c \approx 1.95$  GPa. Homogeneous bulk superconductivity is only observed above this critical pressure. We present a detailed analysis of the influence of pressure inhomogeneities on the specific heat anomalies which emphasizes that the observed broadening of the transitions near  $P_c$  is connected with the first-order transition. For CeCoIn<sub>5</sub> we show that the large specific heat anomaly observed at  $T_c$  at ambient pressure is suppressed linearly at least up to 3 GPa.

## 1. Introduction

Heavy fermion systems provide a unique opportunity to study the interplay of long-range magnetic order, unconventional superconductivity (SC) and valence fluctuations. For usual superconductors the attractive interaction between two electrons forming a Cooper pair is due to a lattice instability and magnetic impurities are pair breaking. The discovery of superconductivity at the verge of an antiferromagnetic ordered state in cerium heavy fermion

systems like CeCu<sub>2</sub>Si<sub>2</sub> [1], CeCu<sub>2</sub>Ge<sub>2</sub> [2], CeRh<sub>2</sub>Si<sub>2</sub> [3] CePd<sub>2</sub>Si<sub>2</sub> and CeIn<sub>3</sub>[4] suggested a pairing mechanism associated with the magnetic instability. The importance of critical valence fluctuations for the appearance of SC in systems with strong electronic correlations has been pointed out recently [5, 6].

The discovery of superconductivity in CeMIn<sub>5</sub> (M = Co, Rh, Ir) compounds opened new routes to investigate the appearance of pressure-induced SC in heavy fermion compounds and its interplay with antiferromagnetism (AFM) [7–9]. While CeCoIn<sub>5</sub> and CeIrIn<sub>5</sub> are superconductors at ambient pressure with superconducting transition temperatures  $T_c = 2.3$  and 0.4 K, CeRhIn<sub>5</sub> is antiferromagnetically ordered below the Néel temperature  $T_N = 3.8$  K and SC appears only under hydrostatic pressure. The family of CeMIn<sub>5</sub> is closely related to CeIn<sub>3</sub> and the crystal structure consists of alternating layers of CeIn<sub>3</sub> and MIn<sub>2</sub> stacking along the [001] direction. Due to its cubic structure, CeIn<sub>3</sub> is a nice model system to study the appearance of superconductivity at a quantum critical point where the magnetic order is suppressed, however SC appears only below 0.2 K in the pressure range of 2–3 GPa and the interplay between AFM and SC is experimentally difficult to investigate [4, 10]. The superconducting transition temperatures in CeCoIn<sub>5</sub> and CeRhIn<sub>5</sub> are enhanced by a factor of almost 10 in comparison to CeIn<sub>3</sub>. For superconductivity mediated by spin fluctuations, a higher  $T_c$  is expected for systems with lower dimensionality [11–13] and indeed, in the 115 family, the Fermi surface is almost two-dimensional [14].

The pressure–temperature phase diagram of CeRhIn<sub>5</sub> has already been studied by resistivity  $\rho$  [15], specific heat  $C$  [16], magnetic susceptibility  $\chi$ , nuclear quadrupole resonance (NQR) [17–21], and neutron scattering experiments [22–25]. CeRhIn<sub>5</sub> orders at ambient pressure in an incommensurate antiferromagnetic helical structure with a wave vector  $\mathbf{q} = (0.5, 0.5, 0.297)$  and a staggered moment of about  $0.8\mu_B$ . Contrary to the first measurements [24], recent neutron scattering measurements show no significant change of the magnetic structure and the magnetic moment up to 1.7 GPa [25]. However, an NQR study shows that the internal magnetic field decreases linearly with pressure and slowly approaches a value of about 5% at ambient pressure of 1.75 GPa [18–20]. The difference between neutron and NQR experiment is generally considered to be due to the different time scales of the measurements. From all measurements, except the very first by Hegger *et al*, it follows that the antiferromagnetic order is suppressed near 2 GPa. Only the specific heat experiments [16] found some anomaly above  $T_c$  at 2.1 GPa: nevertheless, AFM order was discarded as a possible origin for that anomaly [16]. SC has been found with transport measurements in the pressure range from 1 to 8 GPa, with the maximum transition temperature  $T_c \approx 2.2$  K at  $P \approx 2.5$  GPa [15]. For pressures  $P > 2$  GPa, CeRhIn<sub>5</sub> would be an unconventional superconductor with line nodes in the gap as shown by measurements of the NQR relaxation rate  $1/T_1$  which has a  $T^3$  dependence below  $T_c$  [17, 18], in agreement with specific-heat measurements [16]. In the intermediate-pressure region between 1.6 and 2 GPa, AFM and SC have been claimed to coexist, with possible ‘extended gapless’ regions in the superconducting gap function. Recent NQR measurements claim to confirm this possibility of gapless superconductivity in the coexistence regime from the observation of a constant  $T_1 T$  below  $T_c/2$ , ascribed to a finite quasiparticle density of states [21].

CeCoIn<sub>5</sub> is a unconventional SC most probably with a d-wave symmetry and line nodes in the gap [17, 26–29]. At ambient pressure, it is located close to an antiferromagnetic quantum-critical point (QCP). Detailed resistivity measurements show that applying hydrostatic pressure tunes the system away from the proximity of the QCP [30, 31]. The huge anomaly observed in specific heat at  $T_c$  at ambient pressure ( $\Delta C/C(T_c) = 4.7$ ) decreases under pressure up to 1.5 GPa [32]. De Haas–van Alphen measurements show cyclotron masses at ambient pressure which are strongly field dependent and which decrease under pressure [33].

In this article we report on detailed ac calorimetric measurements of CeRhIn<sub>5</sub> and CeCoIn<sub>5</sub> in an extended pressure range up to 3.5 GPa. The measurements were performed in argon-loaded diamond anvil cells ensuring almost perfect hydrostatic pressure conditions. The main focus will be on the appearance of SC in the region of coexistence of AFM and SC in CeRhIn<sub>5</sub>. As the physical properties of the 115 family are very sensitive to uniaxial pressure and pressure inhomogeneities [34], the hydrostaticity of the sample environment is very important. Previous specific heat measurements on CeRhIn<sub>5</sub> were performed in a piston cylinder type cell with a solid pressure transmitting medium (AgCl) [16]. Even if the pressure difference along the length of the sample is quite small, the effect of stress on the sample is not negligible. The nature of the superconducting transition in CeRhIn<sub>5</sub> at high pressure will be related to that of CeCoIn<sub>5</sub>. The main result is for CeRhIn<sub>5</sub> the observation of nice specific heat anomalies at the antiferromagnetic transition at low pressure and at the superconducting transition above 2 GPa. Superconductivity appears in specific heat measurements only very close to the critical pressure where both transitions are tiny and rather broad. From the pressure dependence of the superconducting anomaly  $\Delta C/C(T_c)$  it follows that in CeCoIn<sub>5</sub> at ambient pressure, SC sets in when the effective mass of the electrons is still increasing towards low temperatures due to the formation of the heavy fermion state, whereas at 3 GPa it behaves like the usual heavy-fermion superconductor. For both compounds, the effect of pressure inhomogeneities on the magnetic and superconducting transition will be discussed.

Regarding notations, we call  $P_{S-}$  the lowest pressure for which superconductivity is observed,  $P_{S+}$  the highest pressure for which superconductivity is observed, and  $P_c$ , the pressure of the point where the AFM transition line  $T_N(p)$  meets the superconducting transition line  $T_c(P)$ . Let us remind the reader here that the antiferromagnetic state is also labelled ‘AFM’, the superconducting state ‘SC’, a coexisting AFM and SC state ‘AFM+SC’, and the paramagnetic state ‘PM’.

## 2. Experimental details

High-quality single crystals of CeRhIn<sub>5</sub> and CeCoIn<sub>5</sub> have been grown by the In flux method [7]. The specific heat measurements under pressure were performed using ac calorimetry. In the case of CeRhIn<sub>5</sub> we set up two pressure cells giving almost identical results. Details of this technique for measurements of the specific heat are given elsewhere [35–37]. The size of the samples studied was about  $200 \times 200 \times 60 \mu\text{m}^3$ . An AuFe/Au thermocouple served to measure the temperature oscillations of the sample. It is soldered directly on the sample to ensure a good thermal contact between the thermometer and the sample. As a heater we used a 50 mW argon laser. By using a mechanical chopper it is possible to obtain a quasi-sinusoidal power which is transmitted by optical fibre directly to the sample. However, this method does not allow quantitative measurements, as the heating power is not focused on the sample, but irradiates the pressure transmitting medium (argon) and the gasket which are heated and contribute to an additional background signal which changes between different experiments. To find the optimal working frequency  $\nu$ , the frequency dependence of the ac signal was measured at 1.5 and 4.2 K. The cut-off frequency  $\nu_c$  was found to be about 600 Hz, the measurements were performed at 831 Hz slightly above  $\nu_c$ . The specific heat of the sample can be estimated by  $C_{ac} \propto -PS_{th} \sin(\theta - \theta_0)/V_{th}2\pi\nu$ , where  $V_{th}$  and  $S_{th}$  are respectively the measured voltage and the thermopower of the thermocouple. As the origin of the phase  $\theta_0$  cannot be determined by our method, we neglect in the analysis the contribution of the signal phase. However, a comparison of the behaviour of the signal at low pressure with an absolute measurement at ambient pressure shows that the observed ac signal is correct.

The ac susceptibility was measured in an argon-loaded sapphire anvil cell with 2.5 mm culets diameter. Both anvils are placed inside one of the detection coils (5000 turns), the second detection coil is placed above the anvils. In this geometry the sample and the gasket are in the middle of the lower detection coil. This geometry allows a very good compensation of the susceptometer at fixed temperature, however the filling factor is poor. An additional difficulty comes from a temperature drift of the background signal which cannot be compensated. The measurements were performed at 71 Hz, and before each run the susceptometer was offset at the lowest temperature by compensating the amplitude and the phase of the signal with a small compensation coil which is wound directly on the excitation coil. This susceptometer allows the detection of the onset temperature of the superconducting transition due to the diamagnetic shielding, however it is not possible to conclude about the superconducting volume fraction. The total volume of the measured samples was about  $0.01 \text{ mm}^3$ .

In both experiments, the pressure was determined *in situ* at low temperatures by the ruby fluorescence at 4.2 K. A bellow system allows the pressure at low temperature [38] to be changed and fine tuned.

### 3. Specific heat of CeRhIn<sub>5</sub> under pressure

#### 3.1. Experimental results

Temperature dependence of the specific heat signal of CeRhIn<sub>5</sub> is plotted in figure 1 for different pressures. The inset shows the specific heat of CeRhIn<sub>5</sub> at ambient pressure. At  $T_N$ ,  $C/T$  has a very sharp peak at ambient pressure. The entropy connected with the magnetic transition is small, about  $0.3R \ln 2$ . The remaining entropy is recovered up to 20 K. This strong enhancement of the specific heat in the vicinity of  $T_N$  shows the importance of short-range order (magnetic fluctuations) and is not described by mean field theory. In the magnetically ordered state, the specific heat follows  $C/T = \gamma + \beta_M T^2$  below 1.4 K with  $\gamma = 52 \text{ mJ mol K}^{-2}$  and  $\beta_M = 24 \text{ mJ mol K}^{-4}$ . The Sommerfeld coefficient  $\gamma$  is enhanced and the  $T^2$  term indicates the presence of antiferromagnetic spin waves. In comparison to the anomaly at  $T_N$  at ambient pressure, at 0.6 GPa the magnetic anomaly is shifted to higher temperatures and the transition is only slightly broadened. The magnetic ordering temperature  $T_N$  is determined by the maximum of  $C/T$ . With increasing pressure above 0.6 GPa,  $T_N$  decreases and for pressures higher than 1 GPa the transition starts to broaden, however the magnetic anomaly remains well defined. At 1.85 GPa the magnetic anomaly at  $T_N = 2.2 \text{ K}$  is very broad. A second maximum associated with a superconducting transition is observed at lower temperatures at  $T_c = 1.8 \text{ K}$ . Increasing the pressure by only 0.05 GPa leads to a suppression of the maximum at the magnetic transition, and only a shoulder above  $T_c$  points to an antiferromagnetic state. With further increase in pressure, the superconducting transition gets more pronounced and at 2 GPa, slightly above  $P_c = 1.95 \text{ GPa}$ , only a clear superconducting transition is found. In the investigated temperature range  $T > 1.4 \text{ K}$  we see no sign of a magnetic transition above  $P_c$  in the superconducting phase. The superconducting transition increases up to 2.21 K at 2.4 GPa. Increasing the pressure further leads to a suppression of  $T_c$  (see figure 2).

In figure 3 the ac susceptibility signal connected with the superconducting transition is plotted. A superconducting anomaly is first seen at 1.5 GPa, but the width of the transition  $\Delta T_c = 200 \text{ mK}$  is very large. With increase in pressure, the transition width gets smaller and  $T_c$  increases ( $\Delta T_c = 50 \text{ mK}$  at 2.3 GPa) and the maximum  $T_c = 2.21 \text{ K}$  is observed. For  $P < P_c$  and for  $P > 2.5 \text{ GPa}$ , the onset of the superconducting transition by susceptibility ( $T_c^x$ ) is at higher temperatures than the onset of the transition by specific heat ( $T_c^C$ ). A cascade  $T_c^p > T_c^x > T_c^C$  of superconducting transition temperatures determined by resistivity ( $T_c^p$ ), susceptibility and specific heat measurements is characteristic of heterogeneous materials.

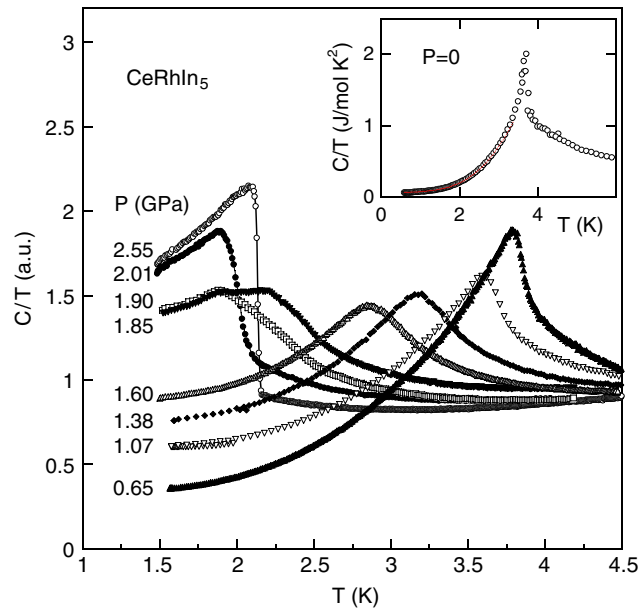


**Figure 1.** Specific heat of CeRhIn<sub>5</sub> for different pressures  $p$  (pressure cell #1). The data are normalized at  $T = 5$  K. The inset shows the specific heat measured at ambient pressure. (This figure is in colour only in the electronic version.)

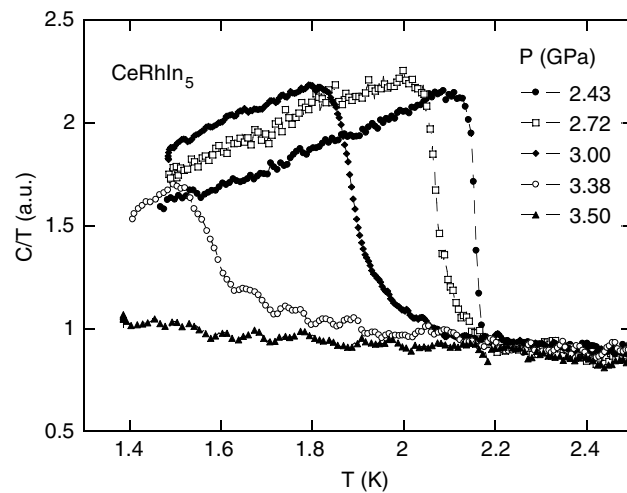


**Figure 2.** Superconducting transition at high pressures for CeRhIn<sub>5</sub> (pressure cell #2).  $C/T$  is normalized in the normal state at  $T = 2.2$  K.

### 3.2. Phase diagram of CeRhIn<sub>5</sub>

In figure 4, we summarize the phase diagram of CeRhIn<sub>5</sub> obtained by specific heat and susceptibility measurements. In addition, we plotted  $T_c$  obtained by resistivity measurements (+) from Llobet *et al* [25]. The phase diagram of CeRhIn<sub>5</sub> can be divided into three different parts: at low pressure,  $P < 0.9$  GPa, the ground state is purely antiferromagnetic. In

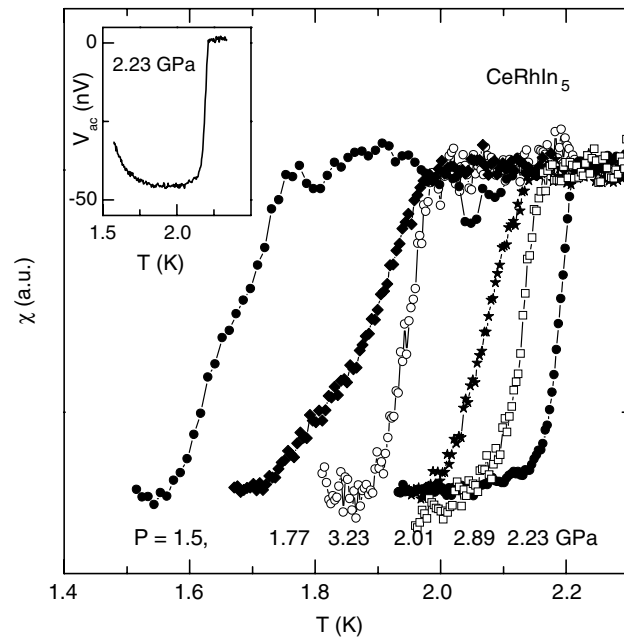


**Figure 3.** Superconducting transition of CeRhIn<sub>5</sub> observed in ac susceptibility. The amplitude of the transition is arbitrary and scaled for different pressures. The onset of the transition is very sharp only above the critical pressure  $P_c = 1.9$  kbar. The inset shows the observed signal in absolute units for 2.23 GPa. The increase of the signal at low temperatures is due to the background.

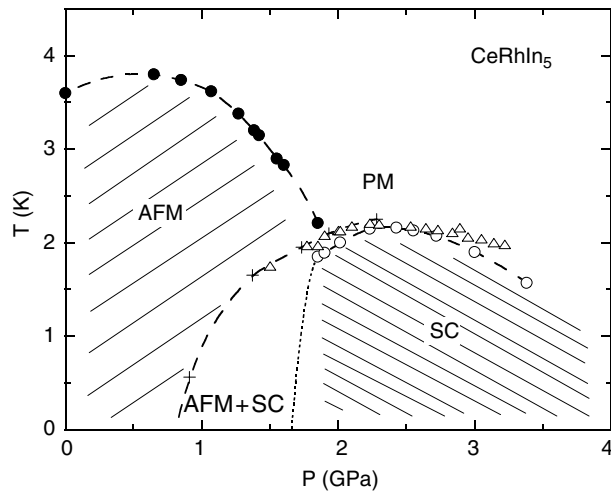


**Figure 4.** Phase diagram of CeRhIn<sub>5</sub> as determined by specific heat (● and ○) and susceptibility measurements (Δ). In addition  $T_c(p)$  from resistivity measurements ( $\rho = 0$ ) after Llobet *et al* [25] is plotted (+). The hatched areas mark the regimes where pure AFM and pure SC states are observed. The dotted line indicates the most probable first order line between the AFM and the SC bulk phase; in the (AFM + SC) regime SC is expected to be only filamentary and not a bulk property.

a limited pressure range  $0.9 \text{ GPa} < P < 1.95 \text{ GPa}$  superconductivity and antiferromagnetism may coexist, and for  $P > 1.95 \text{ GPa}$  the ground state is superconducting. The AFM transition line  $T_N(P)$  meets the SC transition line at  $P_c \approx 1.95 \text{ GPa}$ .

Let us first discuss the AFM transition. At low pressures  $T_N(P)$  first increases with pressure and has a smooth maximum at  $P \approx 0.6 \text{ GPa}$ . In the intermediate pressure range  $0.9 \text{ GPa} < P < 1.95 \text{ GPa}$ ,  $T_N$  decreases monotonically, with a continuously increasing rate exceeding  $2 \text{ K GPa}^{-1}$  at  $P_c$ . Near  $P_c$ , the magnetic transition gets very broad and the amplitude of the magnetic transition is strongly decreasing compared to the low-pressure measurements. These broadening effects will be more quantitatively discussed in the next section. Let us note that both NQR and specific heat measurements agree on the fact that above  $P_c$ , no AFM order is observed: the ground state for  $P > P_c$  is a *pure superconducting state*. When compared with even the latest neutron measurements [25], they do not extend beyond  $1.85 \text{ GPa}$ . However, the strange result (in apparent contradiction with the slow NQR probe ( $10^{-7} \text{ s}$ )) is that the low-temperature ordered moment determined by a quasi-instant probe as neutron scattering ( $10^{-11} \text{ s}$ ) does not collapse with  $T_N$  close to  $P_c$ , but the staggered moment is almost constant up to  $1.85 \text{ GPa}$ .

Switching now to the superconducting transition, the most remarkable fact is the absence of AFM order below  $T_c$  for  $P > P_c$ : the ground state is a pure superconducting state. Nice superconducting anomalies are observed, which become sharper near the maximum  $T_c = 2.2 \text{ K}$  at  $2.55 \text{ GPa}$ . At this pressure, the transition width is comparable to the superconducting transition in CeCoIn<sub>5</sub> at ambient pressure. For higher pressures  $T_c$  determined from the specific heat experiment decreases at the rate of  $-0.7 \text{ K GPa}^{-1}$ . Resistivity measurements by Muramatsu *et al* show that superconductivity is completely suppressed at a pressure  $P_{S+}$  of  $\approx 8 \text{ GPa}$  [15]. Contrary to the previous work [16], we do not observe any rounded anomaly above  $P_c$  due to its normal phase, and *a fortiori* no sign of AFM transition. In agreement with [16], we also do not observe any sign of an AFM transition below  $T_c$ , even very close to  $P_c$ . So in CeRhIn<sub>5</sub>,  $T_N$  is not suppressed continuously to zero, but has a finite value at  $P_c$ . It demonstrates the absence of a quantum critical point in CeRhIn<sub>5</sub>. Thermodynamically, it means that once  $T_c$  is above  $T_N$ , the free energy of the superconducting state is lower than that of the AFM state, whatever the temperature, and that in CeRhIn<sub>5</sub> AFM order and superconductivity compete.

This also has consequences on the pairing mechanism: this competition and the closeness of the energy scales of both phenomenon, makes the AFM correlations as a sole source of the pairing mechanism very unlikely. For example, an extraordinarily strong coupling regime would be required to explain that the maximum  $T_c$  is so close (a factor of  $\approx 2$ ) to the maximum  $T_N$ . Furthermore, the superconducting anomaly  $\Delta C/C(T_c)$  is largest in the pressure range from 2.5 to 3 GPa, pointing to a maximum of the pairing interaction for SC above  $P_c$ . Interestingly, this is the pressure range where the resistivity has a linear temperature dependence above  $T_c$  and the residual resistivity  $\rho_0$  is a maximum as a function of pressure [15]. This may be interpreted as a hint to the probable importance of valence fluctuations in the superconducting pairing mechanism [5].

The regime above  $P_c$  also puts severe constraints on the possible coexistence of a regime below  $P_c$ . In resistivity measurements on high-quality crystals at Los Alamos [25], SC was determined down to much lower pressures than  $P_c$ :  $P_{S-} \approx 0.9 \text{ GPa}$ . The extrapolation of  $T_c \rightarrow 0$  coincides almost with the pressure of the maximum of  $T_N$ . The transition temperatures  $T_c$  determined from the ac susceptibility measurements are in good agreement with these resistivity measurements. However, with ac calorimetry, we find a superconducting anomaly only very close to the critical pressure  $P_c = 1.95 \text{ GPa}$ . This questions the homogeneous coexistence of superconductivity and antiferromagnetism in this pressure range, as the observed

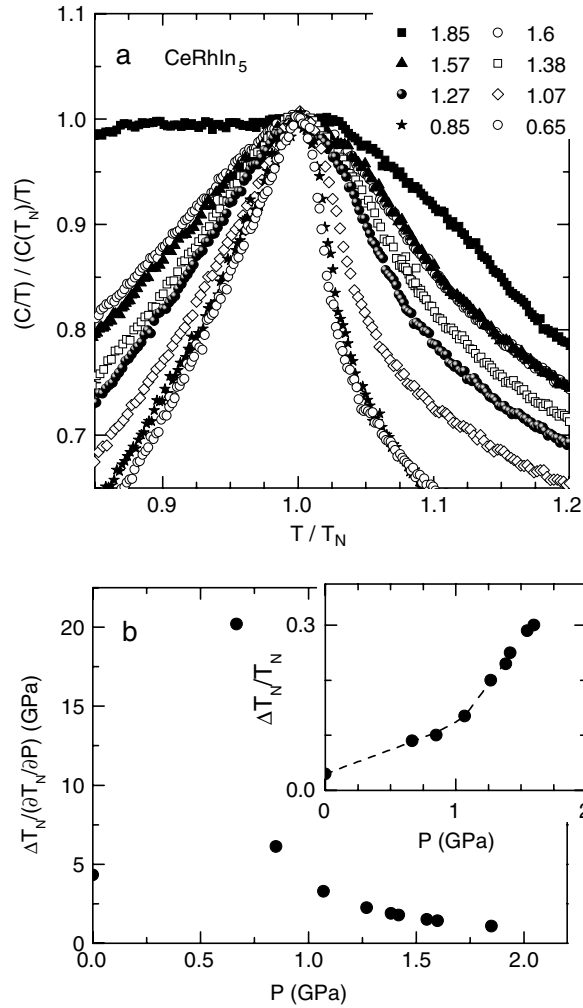


transitions in resistivity and susceptibility are not a bulk probe of superconductivity. From the specific heat measurements, we know that at 1.5 GPa,  $T_c$ , if non-zero, is below 1.5 K. So instead of  $P_{S-} \approx 0.9$  GPa, we expect an almost vertical line between  $P_{S-}$  and  $P_c$ . This would mean that the line  $T_c(P)$  drawn by resistivity or susceptibility measurements within the AFM state does not reflect a bulk transition, and might be connected to internal stress inside the sample, like in CeIrIn<sub>5</sub> [39]. This also means that previous claims of a coexistence of AFM order and superconductivity [21, 25] relying on the observation of AFM order below the resistive  $T_c$  in the pressure range between  $P_{S-}$  and  $P_c$  are not a definite proof of that coexistence. Differences in  $T_c^x$  and  $T_c^C$  are also observed above 2.5 GPa, the pressure where the maximum  $T_c$  occurs. Of course, in our scenario of a direct AFM  $\rightarrow$  SC transition, the line between AFM and SC is expected to be a first-order line, owing to the sudden disappearance of the magnetic order parameter (and in agreement with the strong slope of  $|\partial T_c/\partial P|$ ). Further intrinsic phase separation with a mixed phase may be possible. In CeIn<sub>3</sub>, phase separation was nicely demonstrated by NQR [40].

To summarize this discussion, from our specific heat and ac susceptibility measurements, two different scenarios are possible; (i) the appearance of superconductivity in the antiferromagnetically ordered state is not homogeneous and no true AFM + SC state exists. The experimental observations would then result from superconducting filaments, which can be created due to internal stress induced by dislocations or stacking faults, or due to a phase segregation in a pure magnetically ordered and in a superconducting volume fraction. With increasing pressure, the antiferromagnetic volume decreases and the paramagnetic volume which has a superconducting ground state increases. Above  $P_c$ , only the superconducting state survives. (ii) The coexistence is really homogeneous, which means that the same electrons are responsible for the antiferromagnetic order and for superconductivity. In this case, the missing anomaly of the superconducting transition in the specific heat is due to a gapless superconducting state which is not explained by impurities, and the coexistence phase corresponds to a new class of superconducting states [41]. In the following, both possibilities will be discussed, although we strongly believe in the first scenario.

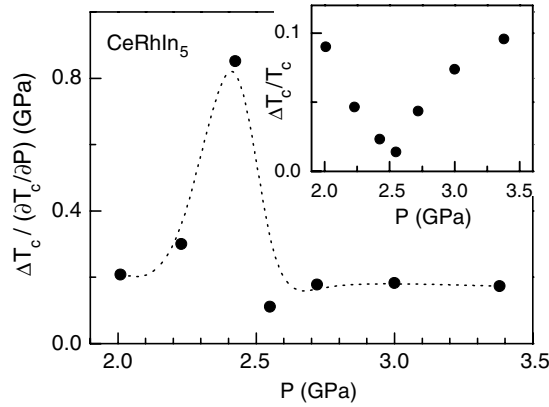
### 3.3. On the transition broadening

Figure 5(a) shows the specific heat in a normalized representation  $C(T)/T/(C(T_N)/T)^{-1}$  as a function of  $T/T_N$ . To quantify the observed broadening of the magnetic anomaly, we arbitrarily define the full width of the transition when  $C(T)/T/(C(T_N)/T)^{-1} = 0.8$ . The relative width of the antiferromagnetic transition as a function of pressure is then shown in the inset of figure 5(b). A change of regime is clearly visible at 0.9 GPa where  $T_N$  starts to decrease and superconductivity is observed by Llobet *et al* [25]. At low pressure the anomaly is rather sharp, but for  $P > 0.9$  GPa it gets continuously broader. However, several effects come into play. Part of the width is intrinsic, coming from the fluctuations, and it is expected to yield a constant value of  $\Delta T_N/T_N$ . In addition, material inhomogeneities, internal or external stress, pressure gradients, might give a pressure-dependent contribution to  $(\Delta T_N/T_N)$ . Some of these effects will be proportional to the pressure variation of  $T_N$  and so to  $\partial T_N/\partial P$  in a first approximation (see figure 5(b)). Detailed measurements show that the pressure variation in a diamond anvil cell with argon in the low-pressure range ( $P < 6$  GPa) is generally lower than 0.04 GPa [42]. Considering the width and also the shape of the ruby spectra, we could not detect any significant broadening of these spectra over the whole investigated pressure range. If the observed broadening resulted only from pressure inhomogeneities in the pressure cell, this would require pressure inhomogeneities of the order of 0.055 GPa near  $P_c = 1.95$  GPa, which can be excluded.



**Figure 5.** (a) Specific heat anomaly due to the antiferromagnetic order of CeRhIn<sub>5</sub> normalized by the maximum of  $C/T$  at  $T_N$  as a function of  $T/T_N$ . (b) The transition width  $\Delta T_N$  normalized by the slope of the variation of  $T_N$  versus  $p$ . The width of the transition is arbitrarily taken at  $(C(T)/T)/(C(T_N)/T) = 0.8$ . The inset shows the relative width of the antiferromagnetic transition  $\Delta T_N/T_N$  observed in the specific heat experiment as a function of pressure.

Further, the very sharp superconducting transition observed at 2.4 and 2.55 GPa in different pressure cells are *a posteriori* a strong indication of high hydrostaticity. Here the width of the transition,  $\Delta T_c = 3$  mK, is comparable to the superconducting transition of CeCoIn<sub>5</sub> at ambient pressure (see below). This clearly shows that the broadening of the magnetic transition on approaching the critical point is not related to the pressure cell. Similar behaviour has been observed in other heavy fermion systems like CeIn<sub>3</sub> [10], CePd<sub>2</sub>Si<sub>2</sub> [43] and CeRh<sub>2</sub>Si<sub>2</sub> [44] too. Theoretically, in the case of a second-order phase transition which ends at the critical pressure  $P_c$ , the form of the mean-field magnetic transition for  $T_N \rightarrow 0$  is sharp. Only the size of the anomaly should decrease as the ordered magnetic moment decreases [45], which is not even the case in CeRhIn<sub>5</sub> [25]. Regarding impurity effects, in the classical framework of



**Figure 6.** Width of the superconducting transition in CeRhIn<sub>5</sub> in the ac calorimetry normalized by the slope of  $T_c$  versus  $P$ . It is basically constant, the high point at  $P_c$  coming from the residual finite width divided by a vanishing  $\partial T_c / \partial P$ . Inset: relative width of the superconducting transition from specific heat experiments in CeRhIn<sub>5</sub> as a function of pressure.

a second-order phase transition (Harris criterion [46]), they are believed to change the critical behaviour only if the specific heat diverges at  $T_N$ .

Here the phenomenon is quite different and more similar to surface problems found in magnetism or for some local structural transitions. Physically, it seems that the magnetic coherence length at  $T_N$  cannot exceed a critical value  $\xi_c$ . For  $P \rightarrow P_c$  the magnetic coherence length at  $T \rightarrow 0$  will increase strongly, there is a severe cut-off in the development of a large coherence length and thus in a corresponding smearing of the specific heat anomaly.

In the pressure range of a first-order transition the entropy drop  $\Delta S$  associated to the magnetic transition is linked to the slope of  $\partial T / \partial P$  according to the Clapeyron relation  $\partial T / \partial P = \Delta V / \Delta S$ , where  $\Delta V$  is the volume discontinuity. The final vertical slope of  $\partial T / \partial P$  as  $T \rightarrow 0$  reflects the collapse of the entropy in agreement with the Nernst principle. As the material is highly sensitive to imperfections, the entropy drop corresponds to a broad specific heat anomaly. The corresponding entropy contribution  $\Delta S$  reflects the amplitude of  $\partial T / \partial P$ , since by contrast the volume discontinuity may change weakly under pressure. So it is quite reasonable that the specific heat anomaly of the magnetic transition disappears drastically on approaching  $P_c$ .

Internal stress may lead to drastic effects as antagonistic behaviours are often observed in the variation of the Néel temperature for a strain  $\sigma$  applied in non-equivalent directions. Well known examples for tetragonal systems are CePd<sub>2</sub>Si<sub>2</sub> [47, 48] or URu<sub>2</sub>Si<sub>2</sub> [49, 50]. In the latter, the values at ambient pressure are:  $\partial T_N / \partial \sigma_a = +900 \text{ mK GPa}^{-1}$  and  $\partial T_N / \partial \sigma_c = -410 \text{ mK GPa}^{-1}$  for  $T_N = 17 \text{ K}$ . The strain dependence of  $T_c$  in URu<sub>2</sub>Si<sub>2</sub> illustrates the antagonism between magnetism and superconductivity as the respective variations of  $T_c$  and  $T_N(\sigma)$  are opposite:  $\partial T_c / \partial \sigma_a = -620 \text{ mK GPa}^{-1}$  and  $\partial T_c / \partial \sigma_c = +430 \text{ mK GPa}^{-1}$  for  $T_c = 1.2 \text{ K}$ . Huge effects have also been detected in the pressure dependence of  $T_N$  in CePd<sub>2</sub>Si<sub>2</sub> measured on two crystals with the  $c$  axis parallel or perpendicular to the pressure gradient due to the non-hydrostaticity of the pressure cell [48]. Of course, as the superconducting domain is locked at  $P_c$ , a large difference appears also in  $T_c(P)$ . To summarize, the broadening is strongly associated to the magnitude of  $\partial T_N / \partial P$  and thus the calorimetric anomaly collapses at  $P_c$ .

In figure 6 the transition width of the superconducting transition above  $P_c$  is shown as a function of pressure, and in figure 5 that of the AFM transition below  $P_c$ . In this system, due to the competition between AFM and SC order, we rather expect that these respective

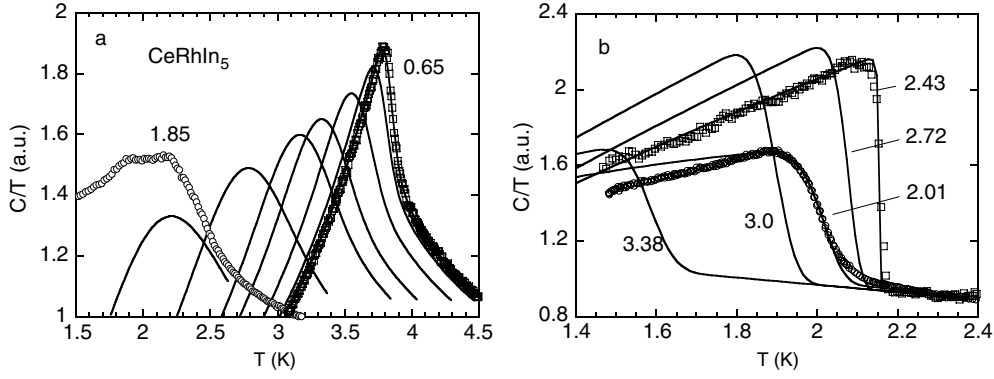


**Figure 7.** (a) Modelling of the specific heat of CeRhIn<sub>5</sub> taking into account a pressure distribution of  $\Delta P = 0.045$  GPa and the slope of  $\partial T_N/\partial p$  for different pressures ( $P = 0.65, 0.85, 1.07, 12.7, 13.8, 1.6$  and  $1.85$  GPa). For comparison, the measured specific heats for  $P = 0.65$  and  $1.85$  GPa are plotted. (b) Effect of the same pressure distribution of  $\Delta P = 0.055$  GPa on the superconducting transition.

transition widths are related to the strength of the pressure variation of their own critical temperature. What is more, in the 115 series, the main source of heterogeneities may be that of internal pressure or strain gradients in the material itself. Thus, local distributions of  $T_c$  or  $T_N$  may be induced. It is well known that near defects like dislocations or stacking faults, internal strain of the order of 0.1 GPa can occur. Evidence for such an effect are given in the paramagnetic state of CeIn<sub>5</sub> at zero pressure as  $T_c^p = 1.2$  K is quite different from  $T_c^C = 0.4$  K [39]. In that case, the superconducting transition observed by resistivity is clearly due to superconducting filaments. This big mismatch of  $T_c$  as measured by resistivity or specific heat seems again directly linked with the difference between  $\partial T_c/\partial \sigma_a = 540$  mK GPa<sup>-1</sup> and  $\partial T_c/\partial \sigma_c = -840$  mK GPa<sup>-1</sup> [34]. Of course an extra cause for heterogeneity can be introduced by the non-hydrostaticity of the pressure transmitting medium. However, in our case, the use of argon optimizes the hydrostaticity.

To demonstrate the impact of internal strain or pressure inhomogeneities when  $\partial T_N/\partial P$  and  $\partial T_c/\partial P$  have a strong pressure dependence, we have calculated the temperature dependence of the specific heat near the antiferromagnetic and the superconducting transition under the assumption of a pressure distribution inside the sample, of width  $\Delta P$ , which may be caused by the experimental conditions or by inhomogeneities in the material. For the antiferromagnetic transition (see figure 7(a)) we suppose that in a hypothetical ideally hydrostatic pressure cell, the shape of the specific heat anomaly would remain unchanged whatever the transition temperature. We have further assumed that at low pressure, the pressure variation of  $T_N$  is small and we can take the curve at 0.65 GPa as the ideal curve. Indeed,  $\partial T_N/\partial P \approx 0$  for 0.65 GPa, so that pressure gradients should have only minor effects on the shape of  $C/T$ . We assume a Gaussian pressure distribution inside the sample, so that the form of the specific heat anomaly for a mean average pressure  $P_0$  is given by

$$\left. \frac{C}{T} \right|_{P_0}(T) = \int \frac{1}{W(P)} \exp \left[ -\frac{1}{2} \left( \frac{P - P_0}{\Delta P} \right)^2 \right] \left. \frac{C}{T} \right|_{0.65} \left( \frac{T}{T_N(P)} \right) dP.$$

The weighting factor  $W$  includes the normalization of the Gaussian distribution, and normalization of  $(C/T)|_{0.65}(T/T_N(P))$  with respect to entropy balance:  $W(P)$  should be proportional to  $T_N$  for localized magnetism, or constant for itinerant magnetism. The difference

in the resulting curves is found to be insignificant for the pressure distribution involved in this experiment. Calculated specific heat transitions for the experimental pressures  $P_0$  and a pressure distribution of  $\Delta P = 0.055$  GPa are shown in figure 7. They have to be compared to the measurements (see figure 1). The broadening in the range where  $\partial T_N / \partial P$  is steep, is clearly visible in the calculations and it is in qualitative agreement with the measurements.

A more quantitative comparison between experiment and these calculations has been done for the superconducting transition, with the same pressure distribution  $\Delta P = 0.055$  GPa. We have calculated the specific heat near the superconducting transition for  $P > 2$  GPa (see figure 7(b)). The entropy balance imposes that  $S_n = S_s$  at  $T_c$  for all pressures. We have assumed a power-law dependence of  $C/T(P) = A(T/T_c)^\alpha$  in the superconducting state<sup>4</sup>, adjusting the exponent  $\alpha$  (which depends on the relative specific heat jump at  $T_c$ ) in order to fulfill the entropy balance. So the calculation of  $C/T$  for a fixed pressure distribution  $\Delta P$  is controlled by two parameters:  $T_c(P)$ , which is known from the phase diagram, and the size of the anomaly at the average pressure (which controls  $\alpha$ ). A comparison with the measurements (see figure 2) shows that the broadening of the transition for pressures below and above the maximum of  $T_c(P)$  can be understood with the same fixed-pressure distribution.

To summarize, a fixed Gaussian pressure distribution of about 0.055 GPa can explain the observed broadening of the antiferromagnetic and the superconducting transitions, as a result of the pressure dependence of  $T_N$  and  $T_c$ . As for the origin of this pressure distribution, 0.04 GPa is really the upper limit expected for inhomogeneities inside a pressure cell filled with argon. More reasonably, these inhomogeneities could be due to internal strain and defects in combination with the anisotropic elastic properties of the material [52].

### 3.4. On the possibility of gapless nature of superconductivity: material effects or novel phase?

The question of a gapless SC state below  $P_c$  started with recent NQR results [21]: just above  $P_c$ , the nuclear relaxation time follows the usual behaviour of an unconventional SC state with line nodes: below  $T_c$ ,  $(T_1 T)^{-1}$  has a nice  $T^2$  dependence. This contrasts with the situation below  $P_c$ . For example at 1.6 GPa, below  $T_c^x$ , at low temperatures  $(T_1 T)^{-1}$  rapidly reaches ( $T \ll T_N$ ), a value corresponding to the normal phase [21]. According to Fisher *et al* [16], the specific heat coefficient  $\gamma$  increases by a factor 3–4, from 0 to 1.6 GPa. This increase in the effective mass leads to an increase in  $(T_1 T)^{-1}$  by one order of magnitude, as observed in the experiment.

We have stressed that our measurements and analysis do not support an intrinsic AFM+SC state between  $P_{S-}$  and  $P_c$ . However, a gapless state in this pressure region could be possible without any additional line in the phase diagram (a continuous evolution of the gap amplitude collapsing on approaching  $P_c$  from the high-pressure region would not necessarily induce symmetry changes). This gapless state cannot be due to impurity scattering, as the criterion for the clean limit is equally satisfied below and above  $P_c$ : the sample investigated in our measurement has a residual resistivity ratio of almost 200 which shows that it is very clean.

The possibility of the realization of p-wave spin singlet superconductivity, whose gap function is odd in frequency and momentum, was very recently discussed by Fuseya *et al* [41]. They showed that near a quantum critical point where strong retardation effects are possible, this p-wave state is more likely than the d-wave state which is expected to be realized away from the critical point in the antiferromagnetic as well as in the paramagnetic regime. A quantum critical point is not observed in our experiment, and a gapless region is also not

<sup>4</sup> As we are only interested in the temperature range very close to  $T_c$ , the correct form of  $C/T$  is not of great importance for the calculation of the broadening of the transition.

observed above  $P_c$  [16]. Nevertheless, this difference might arise from the first-order nature of the AFM  $\rightarrow$  SC transition. The NQR results were interpreted with a heuristic view in favour of this new class of superconducting phase below  $P_c$  which differs from the usual d-wave pairing [21]. Basically, the bare experimental features are similar to those observed here:  $T_c^p$ , the superconducting onset chosen in resistivity is higher than  $T_c^x$  where diamagnetic shielding is observed.  $T_c^x$  appears to coincide with the temperature where tiny features appear in the temperature variation of  $(T_1 T)^{-1}$  of the inverse product of the nuclear relaxation time  $T_1$  by temperature.

From our point of view, the difficulty with this scenario is both quantitative: it is not expected that  $T_c$  could rise up to  $T_N$  (at  $P_c$ ), and qualitative: switching from a gapless p-wave state below  $P_c$  to a gapped d-wave state above  $P_c$  would involve a symmetry change and thus transform the tricritical point at  $P_c$  to a tetracritical point. We would rather interpret the ‘gapless’ nature of superconductivity observed by NQR as related to the heterogeneities observed in the magnetic transition. However, it is obvious that the debate remains. An important issue is to discuss more deeply the discrepancy between neutron diffraction and NQR measurements in the AFM phase.

#### 4. Superconductivity in CeCoIn<sub>5</sub> under high pressure

The specific heat under high pressure of CeCoIn<sub>5</sub> is shown in figure 8. Up to 1.5 GPa, the anomaly under pressure is almost as sharp as at ambient pressure, whereas at higher pressures the anomaly starts to get broader. The phase diagram obtained from specific heat and ac susceptibility measurements is shown in figure 9. With increase in pressure,  $T_c$  increases with an initial rate of  $0.6 \text{ K GPa}^{-1}$  up to 1.6 GPa, for higher pressure it decreases at the rate of  $0.3 \text{ K GPa}^{-1}$  which is slower than the diminution of  $T_c$  in CeRhIn<sub>5</sub>. The very large jump at ambient pressure in the specific heat  $\Delta C/C(T_c) = 4.5$ , which is the largest found in heavy fermion superconductors, was first interpreted as a hint for strong coupling superconductivity in CeCoIn<sub>5</sub> [26, 32]. The pressure dependence of the jump of the specific heat at  $T_c$  is shown in figure 10. The height of the jump obtained by Sparn *et al* was used to determine the background signal for the ac calorimetry and to normalize the jump obtained by ac calorimetry. The background is about 40% of the measured ac signal in the normal state and it is assumed to be linear in temperature and independent of pressure. By increasing the pressure, the large jump in the specific heat decreases linearly to  $\Delta C/C(T_c) = 1$  at 3 GPa. The reduction of the jump with pressure is clearly an indication of the reduction of the effective mass  $m^*$  with increasing pressure. Neglecting strong coupling effects, the jump of the specific heat normalized to the effective mass  $\Delta C/m^* T_c \propto \text{const}$  must be fulfilled. However, the weakness of strong coupling is justified by the temperature variation of the upper critical field of CeCoIn<sub>5</sub>, which can be expressed in a weak coupling model with strong Pauli limitation. The large jump at ambient pressure is due to the fact that superconductivity sets in when the heavy fermion state is not yet formed and the effective mass is still increasing to lower temperatures. Measurements of the specific heat in field at 5 T parallel to the  $c$  axis show that  $C/T$  increases at the lowest temperatures [9, 51]. The increase of  $C/T$  is a strong indication that CeCoIn<sub>5</sub> at ambient pressure is close to a magnetic instability and the system can be driven through a quantum critical point by applying a magnetic field higher than the upper critical field. By contrast, at 3 GPa superconductivity sets in when the heavy masses are formed and CeCoIn<sub>5</sub> behaves as a usual heavy fermion system. The decrease of the effective mass with pressure has been seen directly by de Haas–van Alphen experiments under high pressure [33].

To estimate the influence of pressure inhomogeneities on the superconducting transition in CeCoIn<sub>5</sub> we calculated the specific heat in the same manner as for CeRhIn<sub>5</sub> (see above).

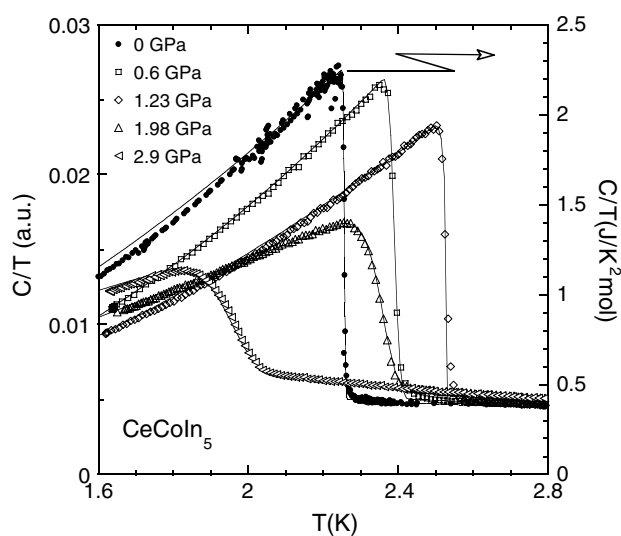


**Figure 8.** Specific heat of CeCoIn<sub>5</sub> under high pressure for different pressures. The ac signal is corrected by a constant background of about 40% of the measured specific heat in the normal state and it is assumed to be linear in temperature and independent of pressure. For comparison,  $C/T$  determined by a quantitative measurement is shown ( $P = 0$ , right scale). Lines are calculations of the specific heat under the assumption of a pressure distribution  $\Delta P$  which increases linearly under pressure from  $\Delta P = 0.015$  for  $P = 0$  up to  $\Delta P = 0.15$  for  $P = 2.9$  GPa.

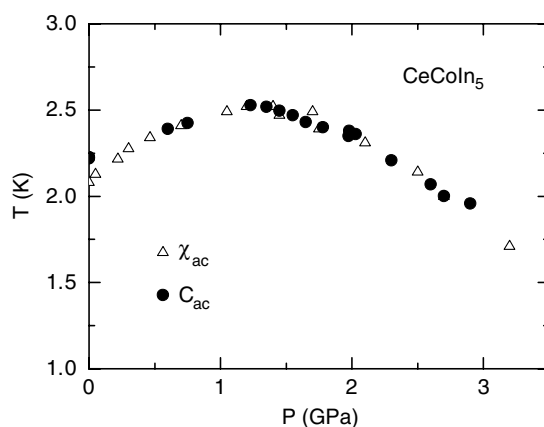


**Figure 9.** Pressure–temperature phase diagram of CeCoIn<sub>5</sub> obtained by high-pressure ac calorimetry (●) and ac susceptibility (△).

However, in addition, the pressure dependence of the effective mass  $m^*$  has to be taken into account. The lines in figure 8 are the results of the calculations. Contrasting with CeRhIn<sub>5</sub>, for CeCoIn<sub>5</sub> the calculated pressure distribution increases linearly from  $\Delta P = 0.015$  GPa at ambient pressure to  $\Delta P = 0.15$  at 2.9 GPa. We can exclude that this increase of inhomogeneity is due to bare pressure gradients. But it could arise from the material itself. As pointed out above, uniaxial stress applied in different crystallographic directions may result in opposite effects on  $T_c$ ,  $\partial T_c / \partial \sigma_a > 0$  and  $\partial T_c / \partial \sigma_c < 0$ . A stress distribution proportional to the pressure

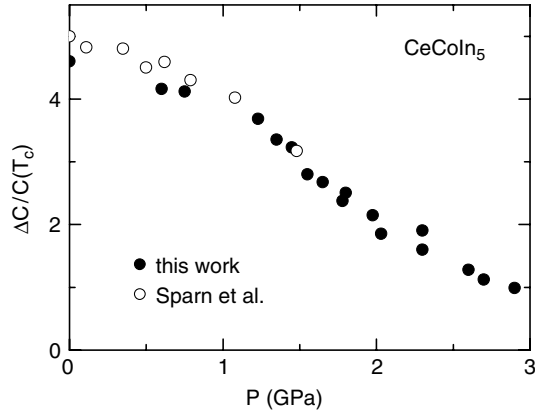


**Figure 10.** Pressure dependence of the jump of the specific heat at  $T_c$  in CeCoIn<sub>5</sub>. (○) From [32] and are used to normalize the jump in the ac calorimetry.

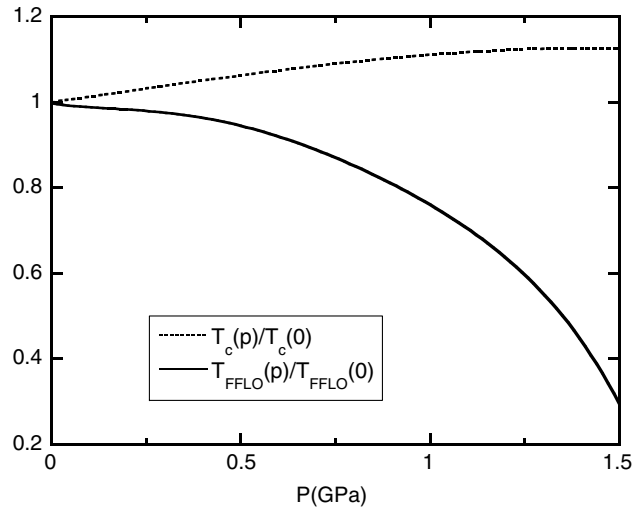


**Figure 11.** Relative evolution of  $T_c(p)$  and  $T_{FFLO}(p)$  as deduced from our measurements of  $T_c(P)$  and of the Sommerfeld specific heat coefficient. Contrary to naive expectations from the rapid drop of  $m^*(P)$ ,  $T_{FFLO}$  is predicted to have only a weak initial pressure variation.

would be the most likely source of this linear increase of  $\Delta P$ . The effect of ‘pressure’ inhomogeneities is expected to be more important in CeCoIn<sub>5</sub> than in CeRhIn<sub>5</sub>, as the anisotropy of the elastic constants of this compound is the largest of the Ce 115 compounds [53].

Recently, the so-called Fulde, Ferrel, Larkin, Ovchinnikov (FFLO) phase has been found in CeCoIn<sub>5</sub> below  $T_{FFLO} < T_c$  close to the upper critical field  $H_{c2}(0)$  for the magnetic field  $H$  applied in the basal plane [54–58]. The key point is that the paramagnetic limit  $H_{c2}^p = 1.8T_c$  in Tesla assuming  $g = 2$  for the conduction electrons governs the behaviour of the upper critical field at very low temperatures since the orbital limit  $H_{c2}^{orb}(0) \approx (m^*T_c)^2$  is far higher than  $H_{c2}^p(0)$ . Nevertheless, the balance between the orbital and paramagnetic limit is expected to change under pressure, due to the variation of  $T_c$  (which controls  $H_{c2}^p$ ) and of  $m^*$ , which controls,



together with  $T_c$ , the  $H_{c2}^{orb}$ . In fact, both  $T_c(P)$  and  $m^*(P)$  are known from our experiment, so we could estimate what should be the relative variation of  $T_{FFLO}$  under pressure in a classical calculation of  $H_{c2}$  including the FFLO state (see for example reference [59]). This is reported in figure 11. From the strong decrease in the effective mass under pressure, we would have expected a drastic decrease of  $T_{FFLO}$  under pressure: this is not the case, due to the initial increase of  $T_c$  which compensates the drop of  $m^*$  with  $P$ . One can predict that  $T_{FFLO}$  will start to decrease significantly only near 1.5 GPa, i.e. when  $T_c$  reaches its maximum, despite the fact that at this pressure,  $m^*$  has decreased by a factor of 2. Of course, this prediction is valid only in a classical scheme: it might be different if for example the interaction itself changes with the magnetic field since the FFLO state appears for magnetic fields just above the field  $H_M$  where pseudo-metamagnetism may occur [58, 60].

## 5. Conclusion

We studied the specific heat of CeRhIn<sub>5</sub> and CeCoIn<sub>5</sub> under high pressure by ac calorimetry and ac susceptibility up to 3.5 GPa. In CeRhIn<sub>5</sub>, a first-order transition from antiferromagnetic order below  $P_c = 1.95$  GPa to a superconducting ground state for  $P > 2$  GPa has been observed. Below  $P_c$ , superconductivity and antiferromagnetism coexist. However, in this regime no superconducting specific heat anomaly has been observed which points to an inhomogeneous appearance of superconductivity in this pressure range. Above  $P_c$  the very sharp superconducting specific heat anomaly is due to homogeneous bulk superconductivity.

The large jump of the specific heat in CeCoIn<sub>5</sub> at the superconducting transition is reduced linearly with increasing pressure. This is a clear indication of the decrease in the effective mass with pressure and the system is tuned away from its magnetic instability. At high pressure, CeCoIn<sub>5</sub> behaves like a usual heavy fermion superconductor.

## Acknowledgments

This work has been supported by the IPMC Grenoble. We thank K Miyake for fruitful discussions.

## References

- [1] Steglich F, Aarts J, Bredl C-D, Lieke W, Meschede D, Franz W and Schäfer H 1979 *Phys. Rev. Lett.* **43** 1892
- [2] Jaccard D, Behnia K and Sierro J 1992 *Phys. Lett. A* **163** 475
- [3] Movshovich R, Graf T, Mandrus D, Thompson J D, Smith J L and Fisk Z 1996 *Phys. Rev. B* **53** 8241
- [4] Mathur N D, Grosche F M, Julian S R, Walker I R, Freye D M, Haselwimmer R K W and Lonzarich G G 1998 *Nature* **394** 39
- [5] Holmes A T, Jaccard D and Miyake K 2004 *Phys. Rev. B* **69** 024508
- [6] Yuan H Q, Grosche F M, Deppe M, Geibel C, Sparn G and Steglich F 2003 *Science* **302** 2104
- [7] Hegger H, Petrovic C, Moshopoulou E G, Hundley M F, Sarrao J L, Fisk Z and Thompson J D 2000 *Phys. Rev. Lett.* **84** 4986
- [8] Petrovic C, Movshovich R, Jaime M, Paglusio P G, Hundley M F, Sarrao J L, Fisk Z and Thompson J D 2001 *Europhys. Lett.* **53** 354
- [9] Petrovic C, Paglusio P G, Hundley M F, Movshovich R, Sarrao J L, Thompson J D, Fisk Z and Monthoux P 2001 *J. Phys.: Condens. Matter* **13** L337
- [10] Knebel G, Braithwaite D, Canfield P C, Lapertot G and Flouquet J 2001 *Phys. Rev. B* **65** 044425
- [11] Monthoux P and Lonzarich G G 2001 *Phys. Rev. B* **63** 054529
- [12] Moriya T and Ueda K 2003 *Rep. Prog. Phys.* **66** 1299
- [13] Fukazawa H and Yamada K 2003 *J. Phys. Soc. Japan* **72** 2449
- [14] Shishido H *et al* 2002 *J. Phys. Soc. Japan* **71** 162

- [15] Muramatsu T, Tateiwa N, Kobayashi T C, Shimizu K, Amaya K, Aoki D, Shishido H, Haga Y and Onuki Y 2001 *J. Phys. Soc. Japan* **70** 3362
- [16] Fisher R A, Bouquet F, Phillips N E, Hundley M F, Pagliuso P G, Sarrao J L, Fisk Z and Thompson J D 2002 *Phys. Rev. B* **65** 224509
- [17] Kohori Y, Yamato Y, Iwamoto Y and Kohara T 2000 *Eur. Phys. J. B* **18** 601
- [18] Mito T, Kawasaki S, Zheng G-q, Kawasaki Y, Ishida K, Kitaoka Y, Aoki D, Haga Y and Onuki Y 2001 *Phys. Rev. B* **63** 220507
- [19] Kawasaki S *et al* 2001 *Phys. Rev. B* **65** 020504 (R)
- [20] Mito T, Kawasaki S, Kawasaki Y, Zheng G-q, Kitaoka Y, Aoki D, Haga Y and Onuki Y 2003 *Phys. Rev. Lett.* **90** 077004
- [21] Kawasaki S, Mito T, Kawasaki Y, Zheng G-q, Kitaoka Y, Aoki D, Haga Y and Onuki Y 2001 *Phys. Rev. Lett.* **91** 137001
- [22] Bao W, Pagliuso P G, Sarrao J L, Thompson J D, Fisk Z, Lynn J W and Erwin R W 2000 *Phys. Rev. B* **62** R14621  
Bao W, Pagliuso P G, Sarrao J L, Thompson J D, Fisk Z, Lynn J W and Erwin R W 2001 *Phys. Rev. B* **63** 219901 (E) (erratum)
- [23] Bao W, Trevino S F, Lynn J W, Pagliuso P G, Sarrao J L, Thompson J D and Fisk Z 2002 *Appl. Phys. A* **74** 557
- [24] Majumdar S, Balakrishnan G, Lees M R, McK Paul D and McIntyre 2002 *Phys. Rev. B* **66** 212502
- [25] Lobet A, Gardner J S, Moshopoulou E G, Mignot J-M, Nicklas M, Bao W, Moreno N O, Pagliuso P G, Goncharenko I N, Sarrao J L and Thompson J D 2004 *Phys. Rev. B* **69** 024403
- [26] Movshovich R, Jaime M, Thompson J D, Petrovic C, Fisk Z, Pagliuso P G and Sarrao J L 2001 *Phys. Rev. Lett.* **86** 5152
- [27] Izawa K, Yamagushi H, Matsuda Y, Shishido H, Settai R and Onuki Y 2001 *Phys. Rev. Lett.* **87** 057002
- [28] Ormeno J R, Sibley A, Gough C E, Sebastian S and Fisher I R 2002 *Phys. Rev. Lett.* **88** 047005
- [29] Aoki H, Sakakibara T, Shishido H, Shishido H, Settai R, Onuki Y, Miranović P and Machida K 2003 *J. Phys.: Condens. Matter* **16** L13
- [30] Nicklas M, Borth R, Lengyel E, Pagliuso P G, Sarrao J L, Sidorov V A, Sparn G, Steglich F and Thompson J D 2001 *J. Phys.: Condens. Matter* **13** L905
- [31] Sidorov V A, Nicklas M, Pagliuso P G, Sarrao J L, Bang Y, Balatsky A V and Thompson J D 2001 *Phys. Rev. Lett.* **89** 157004
- [32] Sparn G, Borth R, Lengyel E, Pagliuso P G, Sarrao J L, Steglich F and Thompson J D 2001 *Frontiers of High Pressure Research II: Application of High Pressure to Low Dimensional Novel Electronic Material* ed H D Hochheimer (Dordrecht, The Netherlands: Kluwer Academic Publishers)
- [33] Shishido H, Ueda T, Hashimoto S, Kubo T, Dettai R, Harima H and Onuki Y 2003 *J. Phys.: Condens. Matter* **15** L499
- [34] Oeschler N, Gegenwart P, Lang M, Movshovich R, Sarrao J L, Thompson J D and Steglich F 2003 *Phys. Rev. Lett.* **91** 076402
- [35] Sullivan P F and Seidel G 1968 *Phys. Rev.* **173** 679
- [36] Demuer A, Marcenat C, Thomasson J, Calemczuk R, Salce B, Lejay P, Braithwaite D and Flouquet J 2000 *J. Low Temp. Phys.* **120** 245
- [37] Wilhelm H and Jaccard D 2002 *J. Phys.: Condens. Matter* **14** 10683
- [38] Salce B, Thomasson J, Demuer A, Blanchard J J, Martinod J M, Devoille L and Guillaume A 2000 *Rev. Sci. Instrum.* **71** 2461
- [39] Bianchi A, Movshovich R, Jaime M, Thompson J D, Pagliuso P G and Sarrao J L 2001 *Phys. Rev. B* **64** 220504 (R)
- [40] Kawasaki S, Mito T, Kawasaki Y, Kotegawa H, Zheng G-q, Kitaoka Y, Shishido H, Araki S, Settai R and Onuki Y 2004 *J. Phys. Soc. Japan* **73** 1647
- [41] Fuseya Y, Kohno H and Miyake K 2003 *J. Phys. Soc. Japan* **72** 2914
- [42] Thomasson J 2004 Private communication
- [43] Demuer A, Sheikin I, Braithwaite D, Fåk B, Huxley A, Raymond S and Flouquet J 2001 *J. Magn. Magn. Mater.* **226–230** 17
- [44] Haga Y *et al* unpublished
- [45] Zülicke U and Millis A J 1995 *Phys. Rev. B* **51** 8996
- [46] Dotsenko V S 1995 *Sov. Phys.—Usp.* **38** 347
- [47] van Dijk N H, Fåk B, Charvolin T, Lejay P and Mignot J M 2000 *Phys. Rev. B* **61** 8922
- [48] Demuer A, Holmes A T and Jaccard D 2002 *J. Phys.: Condens. Matter* **14** L529
- [49] de Visser A, Kayzel F E, Menovsky A A, Franse J J M, van den Berg J and Nieuwenhuys G J 1986 *Phys. Rev. B* **34** 8168

- [50] van Dijk N H, de Visser A, Franse J J M and Menovsky A A 1995 *Phys. Rev. B* **51** 12665
- [51] Bianchi A, Movshovich R, Vekhter I, Pagliuso P G and Sarrao J L 2003 *Phys. Rev. Lett.* **91** 257001
- [52] Kumar R S, Kohlman H, Light B E, Cornalius A L, Raghavan V, Darling T W and Sarrao J L 2004 *Phys. Rev. B* **69** 014515
- [53] Kumar R S, Cornelius A L and Sarrao J L 2004 *Preprint* cond-mat/02405043
- [54] Tayama T, Harita A, Sakakibara T, Haga Y, Shishido H, Settai R and Onuki Y 2002 *Phys. Rev. B* **65** 180504
- [55] Murphy T P, Hall D, Palm E C, Trozer S W, Petrovic C, Fisk Z, Goodrich R G, Pagliuso P G, Sarrao J L and Thompson J D 2002 *Phys. Rev. B* **65** 100514
- [56] Bianchi A, Movshovich R, Oeschler N, Gegenwart P, Steglich F, Thompson J D, Pagliuso P G and Sarrao J L 2002 *Phys. Rev. Lett.* **89** 137002
- [57] Bianchi A, Movshovich R, Capan C, Pagliuso P G and Sarrao J L 2003 *Phys. Rev. Lett.* **91** 187004
- [58] Radovan H A, Fortune N A, Murphy T P, Hannahs S T, Palm E C, Trozer S W and Hall D 2003 *Nature* **425** 51
- [59] Brison J P, Keller N, Verniere A, Lejay P, Schmidt L, Buzdin A, Flouquet J, Julian S R and Lonzarich G G 1995 *Physica C* **250** 128
- [60] Paglione J, Tanatar M A, Hawthorn D G, Boaknin E, Hill R W, Ronning F, Sutherland M, Taillefer L, Petrovic C and Canfield P C 2003 *Phys. Rev. Lett.* **91** 246405